JOURNAL OF SYNCHROTRON RADIATION

Volume 25 (2018)

Supporting information for article:

The fractional Fourier transform as a simulation tool for lens based X-ray microscopy

Anders Filsøe Pedersen, Hugh Simons, Carsten Detlefs and Henning Friis Poulsen

S1. Free choice of sampling examples

Fig. S1 shows the point spread function (PSF) calculated using a 1D square object 10 nm across, using different pixel sizes. It clearly shows that the sampling has no impact on the obtainable PSF.

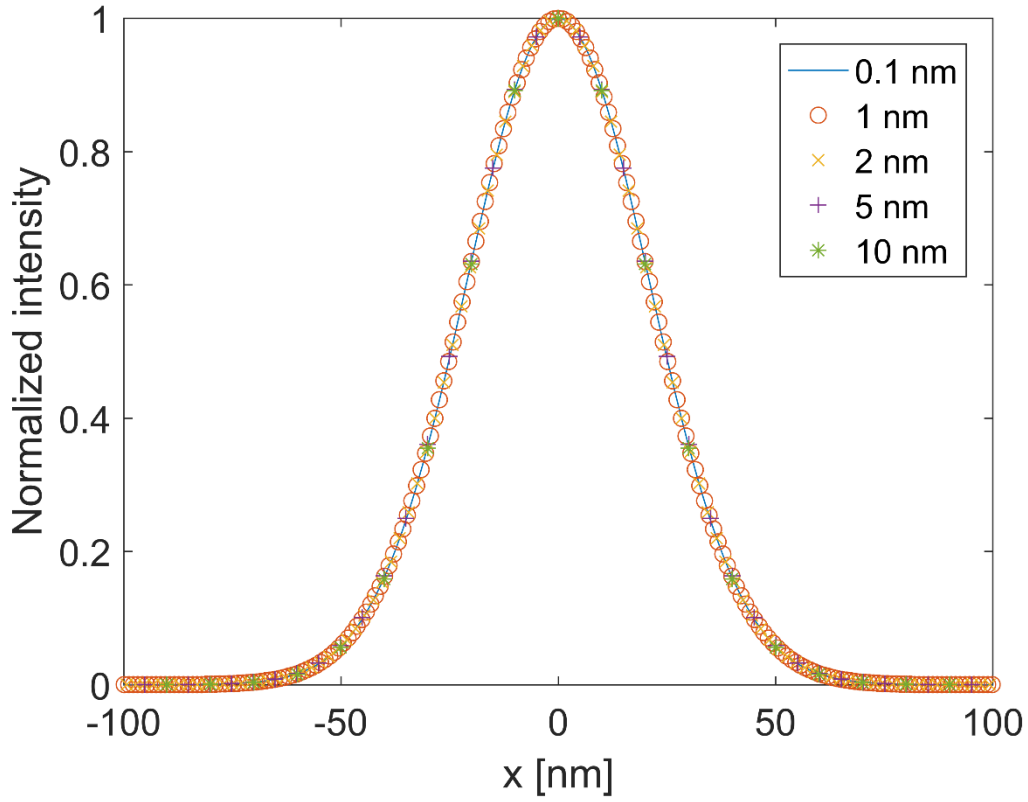

Figure S1 The PSF has been calculated with an effective aperture of the CRL, using a 10 nm square object. The sampling has been varied, and the pixel size is shown in the legend. As expected, the sampling has no effect on the PSF shape. Simulation details: 1D wavefront, constant field of view of 1 µm, see also "Example_Figure_S1.m" in reference (Anders Pedersen, 2017).

Fig. S2 shows a 10 times magnified image of a more complicated test object with a larger field of view. As expected, the difference in sampling has almost no effect on the simulation result. There are small deviations approximately a few percent for the largest pixel size of 1 µm, but in this case there are only 2.5 samples per peak.

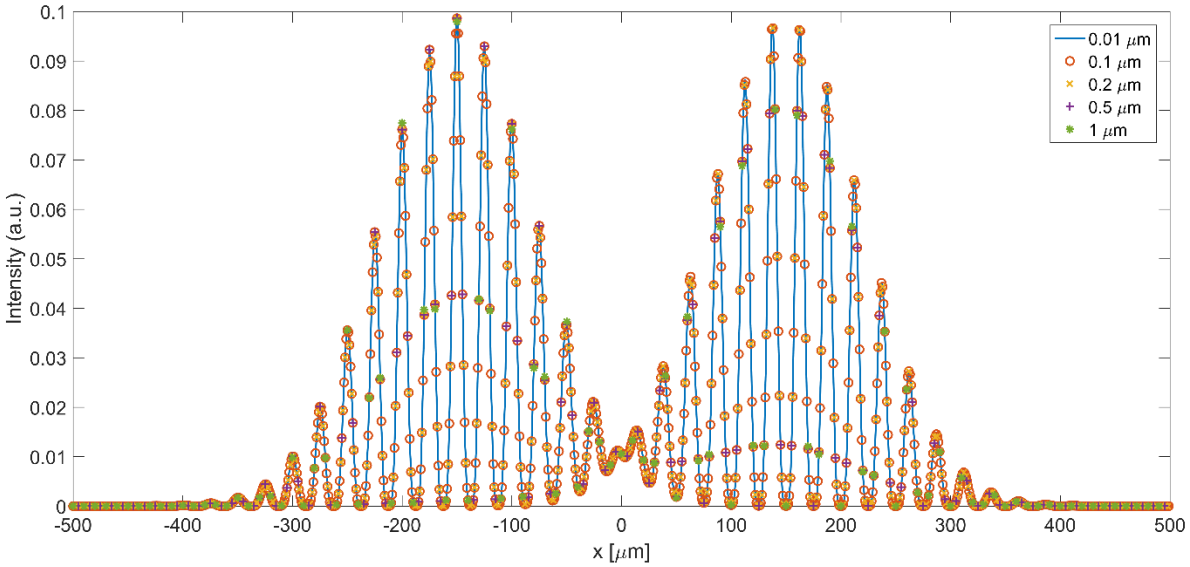

Figure S2 A 10 times magnified image of a more intricate test object has been simulated using different pixel sizes, as indicated in the legend. The different sample sizes all agree. Simulation details: 1D wavefront, constant field of view of 100 μm, see also "Example_Figure_S2.m" in reference (Anders Pedersen, 2017).

S2. Intensity and phase maps

Fig. S3 shows am intensity (a) and phase (b) map of the electric field in the vicinity of the Gaussian PSF.

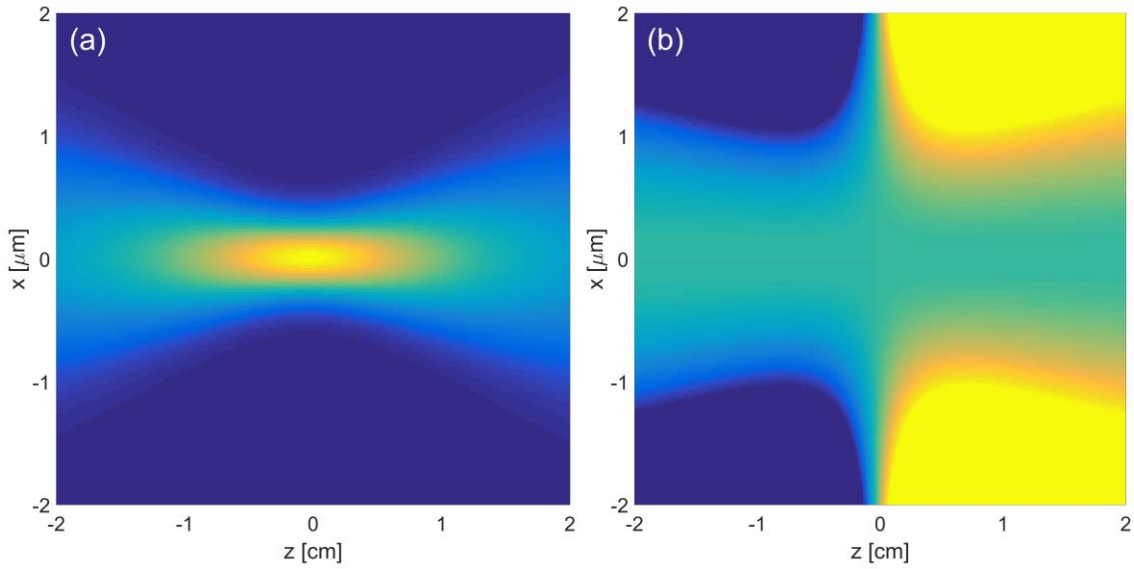

Figure S3 Intensity (a) and phase (b) map of the Gaussian PSF in the vicinity of the image plane. The scale for the phase is [-π;π].

S3. Derivation of analytical expression for effective pupil function

From geometric optics (Simons et al., 2017) we can obtain an effective pupil at the exit of the CRL. Using the FrFT we can then compute the full propagation in just two steps, first propagate through all the lenses to the CRL exit, apply the effective attenuation, and finally propagate to the detector plane. For small objects the attenuation is dominated by the angular attenuation, which has an RMS width of σ_a. Tracing a ray originating on the optical axis with an angle σ_a allows us to obtain the position at the end of the CRL (Eq. (9) in SI of (Simons et al., 2017)):

$$y_N = d_1\sigma_a \cos\left[\left(N-\frac{1}{2}\right)\varphi\right] + f\varphi\sigma_a \sin\left[\left(N-\frac{1}{2}\right)\varphi\right]. \tag{S1}$$

To obtain this expression we set the ray entrance position into the CRL to $y_0 = d_1\sigma_a$. The attenuation (pupil) at the CRL exit is then given by:

$$P(x,y) = \exp\left(\frac{-(x^2+y^2)}{2y_N^2}\right). \tag{S2}$$

S4. Algorithm for calculating effective vignetting width

It is possible to describe the entire signal attenuation from the CRL through the effective pupil function described above and an effective vignetting function in the object plane. This is true in general cases, not only for imaging geometries. Here we describe an algorithm to obtain the RMS width of the Gaussian vignetting function numerically.

We will refer to a "natural" width, which is the RMS width of the attenuation from the CRL assuming parallel beams only:

$$w_0 = \sqrt{\frac{R}{2N\mu}}. \tag{S3}$$

The algorithm is based on fitting the signal at the exit of the CRL, and so we set up a 1D FrFT propagation simulation. The object plane has 100 pixels, a field-of-view of $FOV = 15w_0$, and the object is a box function with a width of $w = 10w_0$. The FrFT parameters are calculates as described in the main manuscript, using the plane of the final lens as the "detector" plane. As a reference, the object is propagated to the exit plane with the physical attenuation in each lens. An optimization function now takes the original object, multiplies it by a Gaussian function with a variable RMS width, propagates it to the CRL exit plane in a single transform, and applies the effective pupil function. The electric field should now be identical to the reference simulation if the vignetting width is correct.

This algorithm is very fast, since the simulation is done in 1D and with only 100 pixels. The optimization algorithm used is the built-in "fminsearch" function in MatLab. The implementation is seen in "Vignetting.m" in reference (Anders Pedersen, 2017).

S5. Derivation of resolution from slit in back focal plane of a CRL

In this derivation, we only look at one dimension, and assuming a square aperture. The other dimension will have an identical resolution. We start by linking the angle in the sample plane to the position in the BFP (Eq. (22) in (Simons et al., 2017)):

$$\alpha_s = \frac{\cos(N\varphi)}{f_N} x_{\mathrm{BFP}}. \tag{S4}$$

Next, we see that the square aperture of full width D only accepts angles up to:

$$\alpha_c = \frac{D\cos(N\varphi)}{2f_N}. \tag{S5}$$

At the critical angle, the maximum spatial acceptance at the CRL entrance is given by:

$$x_{max} = d_1\alpha_c = \frac{d_1 D\cos(N\varphi)}{2f_N}. \tag{S6}$$

In effect, this corresponds to a square pupil function at the CRL entrance:

$$P(x) = \begin{cases} 1, |x| < x_{max}, \\ 0, \text{otherwise}. \end{cases} \tag{S7}$$

From the pupil function, we can derive the unnormalized point spread function (PSF):

$$\begin{aligned} PSF(x) &= \left|\int_{-\infty}^{\infty} P(x_{CRL}) \exp\left(-\frac{2\pi i}{\lambda d_1} x_{CRL} x\right) dx_{CRL}\right|^2 = \left|\int_{-x_{max}}^{x_{max}} \exp\left(-\frac{2\pi i}{\lambda d_1} x_{CRL} x\right) dx_{CRL}\right|^2 \\ &= \left|\frac{\sin\left(\pi \frac{2x_{max}}{\lambda d_1} x\right)}{\pi \frac{1}{\lambda d_1} x}\right|^2 = \left|2x_{max}\,\mathrm{sinc}\left(\frac{2x_{max}}{\lambda d_1} x\right)\right|^2 \\ &= 4x_{max}^2\,\mathrm{sinc}^2\left(\frac{D\cos(N\varphi)}{\lambda f_N}\right). \end{aligned} \tag{S8}$$

The RMS width of a Gaussian fit to the $\mathrm{sinc}^2(ax)$ function is $0.3645/a$, and so the resolution of the slit alone is:

$$\sigma_{\mathrm{slit}} = \frac{0.3645\,\lambda f_N}{D\cos(N\varphi)}. \tag{S9}$$

S6. Computation time and hardware

In the examples in this paper, the propagations have been calculated using a workstation PC equipped with an 8-core 16-thread Intel Xeon E5-1680v4 at 3.40 GHz, an NVidia Titan X (Pascal) GPU, and 128 GB RAM. Fast 2D implementations of the FrFT have been implemented on both the CPU and GPU. For the Saturn image in Fig. 6 of 1200x1500 pixels, a single 2D propagation step takes about 0.28 s on the GPU and 2.4 s on the CPU. On a random 1024x1024 array, a standard 2D FFT is computed in about 0.016 s, whereas the FrFT of the same array is completed in 0.12 s on the GPU and 1.1 s on the CPU.

On a picture of the same pixel number a single propagation step is faster using normal Fourier optics, but in many cases of physical propagation the FrFT will be much faster, let alone feasible, as the number of pixels can be drastically reduced. Furthermore, using the effective aperture for a CRL with N lenses, the full propagation can be completed in 2 propagation steps rather than N+1 steps, which in this case is 35 times faster.